Solid-State Electronics 194 (2022) 108339

Contents lists available at ScienceDirect

Solid State Electronics

journal homepage: www.elsevier.com/locate/sse

Statistical device simulations of III-V nanowire resonant tunneling diodes as physical unclonable functions source

Ali Rezaei [a,*], Patryk Maciazek [a], Amretashis Sengupta [b], Tapas Dutta [a], Cristina Medina-Bailon [a,c], Asen Asenov [a], Vihar P. Georgiev [a,*]

[a] Device Modelling Group, James Watt School of Engineering, University of Glasgow, Glasgow G12 8QQ, United Kingdom
[b] Department of Physics, School of Applied Sciences, REVA University, Bengaluru 560064, India
[c] Nanoelectronics Research Group, Departamento de Electronica y Tecnologia de Computadores, University of Granada, 18071 Granada, Spain

ARTICLE INFO

Keywords:
Resonant tunneling diodes (RTDs)
Physically unclonable function (PUF)
Quantum device simulator
Nano-electronic simulation software (NESS)

ABSTRACT

In this paper, utilising the non-equilibrium Green's function (NEGF) formalism within the new device simulator NESS (Nano-Electronic Software Simulator) developed at the University of Glasgow's Device Modelling Group, we present quantum mechanical simulations of current flow in double-barrier III-V GaAs-AlGaAs nanowire resonant tunneling diodes (RTDs). NESS is a fast and modular Technology Computer Aided Design (TCAD) tool with flexible architecture which can take into account various sources of statistical variability in nanodevices. The aim of this work is to show that, in the RTD devices with nano-scale dimensions, there is a direct correlation between the position and the numbers of random dopants and the key device parameters, e.g., position of the resonant-peak (V_R) variations as well as the shape and number of peaks in the output current–voltage (I-V) characteristics. Such V_R variability can be used as a quantum fingerprint which can provide robust security and hence can be used to deliver Physical Unclonable Functions (PUFs).

1. Introduction

The RTDs are semiconductor quantum well (QW) structure nano-devices with finite rectangular barriers which have negative differential resistance (NDR) in their I-V characteristics. Owing to the presence of this unique NDR property and their relatively simple structure and fabrication process, the RTDs are competitive candidates for interesting digital and analog circuits applications. For example, terahertz (THz) communications is an emerging area related to 5-6G technology development. Due to the ultra-high frequency capabilities, the RTDs are also a very promising choice for wireless and optical resonant THz frequency generation and detection [1–4]. Moreover, the so-called PUFs [5], which are nano-sized devices, have drawn an enormous amount of interest for hardware authentication in cybersecurity applications [6–8]. PUFs can be added to an already existing integrated circuit design to generate a unique output that is determined by material parameters and the structural characteristic, which cannot be duplicated or cloned. Recently, the RTDs have been proposed as the main building blocks for quantum-confinement-based physically unclonable functions (QC-PUFs) [9,10].

Here, we present a numerical investigation of the important role of the random dopant fluctuations (RDFs) variability in the RTDs, showing that the locations of the resonance peaks for each RTD devices are unique, random, and extremely difficult to predict, which indeed makes them suitable for PUFs generation and cryptographic purposes.

2. Simulation methodology

Time and cost-effective computer simulation tools pave the way to experimental electronic device fabrication as they provide deep insight into the physics of device operation. The simulations presented in this work are performed self-consistently utilizing the NEGF solver of our Nano-Electronic Simulation Software (NESS) framework [11–15]. NESS is designed to simulate quantum charge transport in ultra-scaled nano-electronic devices using various integrated solvers such as NEGF, drift–diffusion, and Kubo-Greenwood formalism where the corresponding transport modules are solved self-consistently within the Poisson equation. The NEGF solver implemented in NESS allows us to capture the detailed physical picture of the quantum mechanical effects such as quantum confinement, coherence, particle–particle interactions,

* Corresponding authors.
E-mail addresses: ali.rezaei@glasgow.ac.uk (A. Rezaei), vihar.georgiev@glasgow.ac.uk (V.P. Georgiev).

https://doi.org/10.1016/j.sse.2022.108339
Received 24 March 2022; Received in revised form 14 April 2022; Accepted 19 April 2022
Available online 28 April 2022

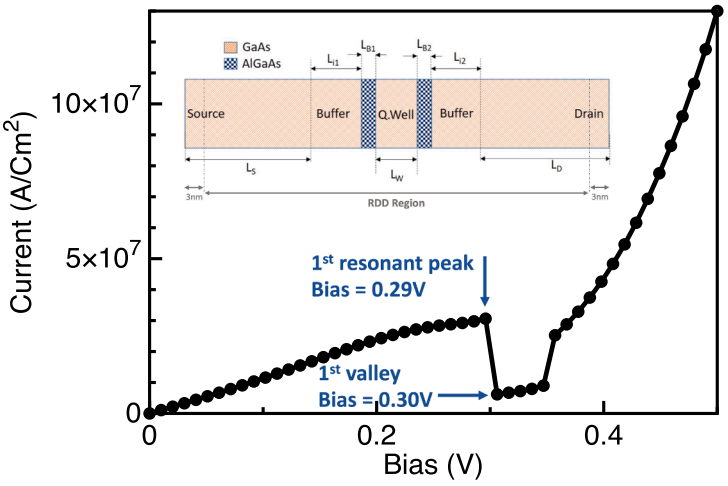

Fig. 1. The I-V characteristic of the baseline GaAs-$Al_{0.3}Ga_{0.7}As$ RTD device and the positions of the first resonant-peak (V_R=0.29 V) and the first valley (V = 0.30 V). The inset depicts its schematic illustration where L_S=L_D=19 nm, L_{i1}=L_{i2}=3 nm, L_{B1}=L_{B2}=3 nm, and L_W=5 nm. The device has a square cross-section of 10 nm × 10 nm, and the total length is 55 nm.

and resonant tunneling of electrons through barriers in structures under investigation. The charge density, potential profile, and the current flow in the system are obtained by performing a self-consistent solution of the Poisson equation and the NEGF transport equations in the coupled mode-space representation. We can either study the transport in (i) pure ballistic limit, (ii) include acoustic or g-type optical electron–phonon scattering mechanisms with the self-consistent Born approximation approach, or (iii) incorporate surface roughness scattering within our NEGF. Moreover, NESS can introduce various sources of statistical variability, e.g., RDF, Line Edge Roughness (LER), or Metal Gate Granularity (MGG).

The NEGF formalism is a widely applied framework for analyzing the quantum transport in mesoscopic and nanoscale devices. Having the system in steady state, one has to solve first at each energy E the relevant components of the retarded G^R, advanced G^A and the lesser Green's function $G^<$, which are governed by the following system of equations [16]

$$G^R(\mathbf{r},E) = \left[(E+i\eta)\cdot\mathbb{1} - \mathbb{h}(\mathbf{r}) - \Sigma^{\mathbb{R}}(\mathbf{r},\mathbb{E})\right]^{-1}, \tag{1}$$

$$G^A(\mathbf{r},E) = \left[G^R(\mathbf{r},E)\right]^{\dagger}, \tag{2}$$

$$G^{\lessgtr}(\mathbf{r},E) = G^R(\mathbf{r},E)\cdot\Sigma^{\lessgtr}(\mathbf{r},E)\cdot G^A(\mathbf{r},E). \tag{3}$$

Where E, $\mathbb{1}$, η, and Σ^R ($\Sigma^{\lessgtr}$) are the energy, identity matrix, an infinitesimal positive real number, and retarded (lesser/greater) self-energies, respectively. The above-mentioned self-energies take into account scattering of the electrons and their interaction with the contacts. The electrons are described in this solver by an effective mass approximation. The one-particle Hamiltonian, h(**r**), reads

$$h(\mathbf{r}) = -\frac{\hbar^2}{2}\frac{\partial}{\partial x}\left(\frac{1}{m_x}\frac{\partial}{\partial x}\right) - \frac{\hbar^2}{2}\frac{\partial}{\partial y}\left(\frac{1}{m_y}\frac{\partial}{\partial y}\right) - \frac{\hbar^2}{2}\frac{\partial}{\partial z}\left(\frac{1}{m_z}\frac{\partial}{\partial z}\right) + U(\mathbf{r}), \tag{4}$$

where, $U(\mathbf{r})$ is the external applied electrostatic potential at position $\mathbf{r} = (x,y,z)$. The semiconductor band-structure is captured by the effective masses along the x,y, and z directions - namely m_j with $j = x,y$, and z. Employing the retarded Green's function component, we can obtain the charge [17,18]

$$n(\mathbf{r}) = \frac{-i}{2\pi}\int dE G^<(\mathbf{r},\mathbf{r}';E), \tag{5}$$

and the current through the l^{th} layer as

$$j(l) = \frac{2|q|}{\hbar}\int \frac{dE}{2\pi}\mathrm{Tr}[2\Re(h_{l+1,l}\cdot G^<_{l,l+1})], \tag{6}$$

where $h_{l+1,l}$ ($G^<_{l,l+1}$) is representing the matrix elements of the Hamiltonian ($G^<$) between the basis states on layer l+1 (l) and l (l + 1).

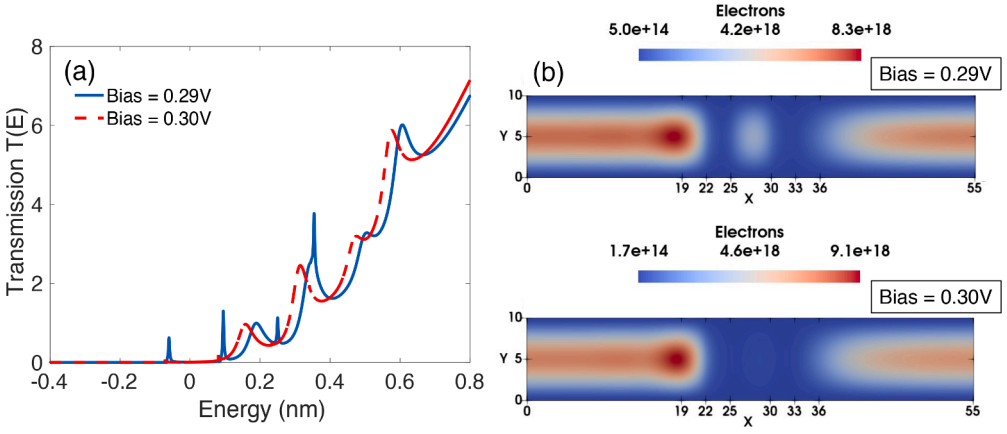

Fig. 2. (a) The comparison of the transmission spectra for V_R=0.29 V and V = 0.30 V. (b) The charge distribution in the XY cut-plane of the device for the 1st resonant-peak (top) and the first valley (bottom).

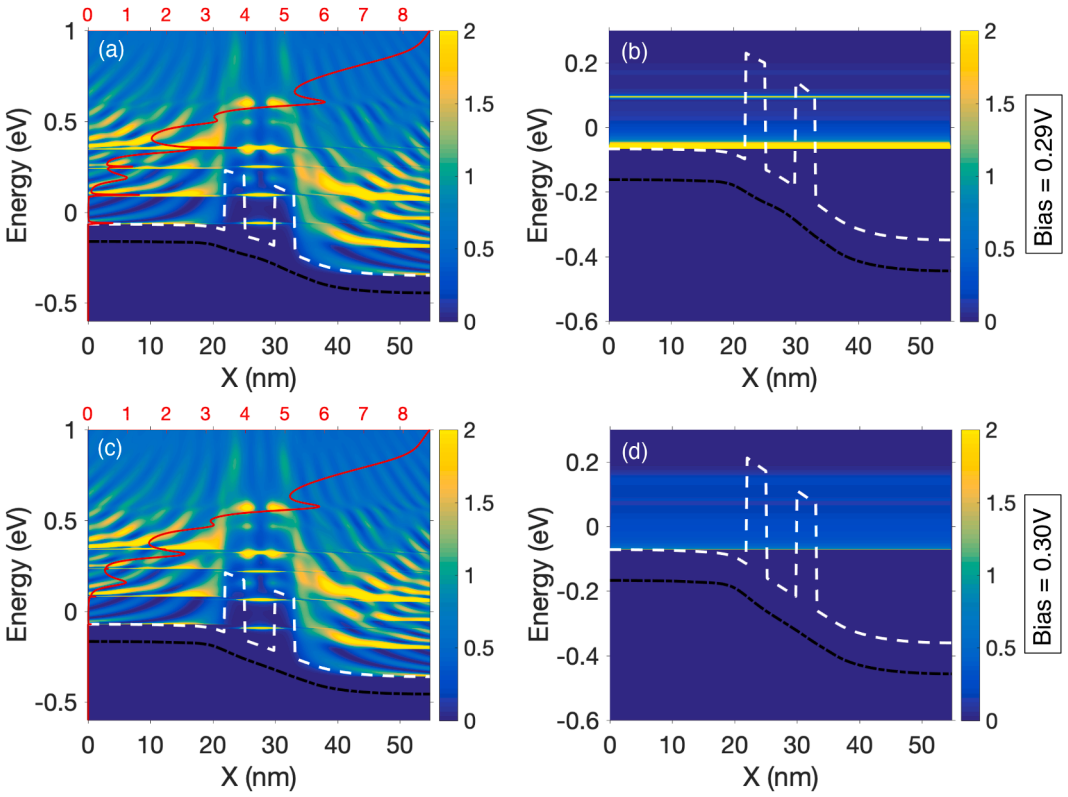

Fig. 3. (a)–(c) The LDOS, potential, first sub-band, and T(E), and (b)–(d) the energy-resolved current spectra of the device at the first resonance peak and the first valley. The red, white dashed, and black lines display transmission, energy sub-band structure, and average potential, respectively. Where, X is the transport direction.

3. Results and discussions

The inset of Fig. 1 shows the simulated double barrier III-V RTD. At the central region of the device, we consider two 3 nm thick regions ($L_{B1,B2}$) made of $Al_{0.3}Ga_{0.7}As$ as the tunneling barriers, enclosing a 5 nm GaAs section (L_W) which serves as the QW. These are separated from the source and drain ($L_{S,D}$) by 3 nm buffer regions ($L_{i1,i2}$). The source and drain regions are n-type doped with a high doping concentration of $2 \times 10^{18} cm^{-3}$, whereas the rest of the device has intrinsic doping.

As depicted in Fig. 1, the current through the RTD rises steadily to reach the first resonant-peak at a bias of 0.29 V, followed by a sharp drop in current down to the first valley at 0.30 V. Such current profile is know as the negative differential resistance (NDR). By applying bias, three distinct regions are formed within the I-V characteristic. For low biases, the first confined state (resonant state) between potential barriers gets closer to the source Fermi level as bias increases, therefore, the current it carries increases. Further increasing the bias makes the first confined state lower in energy, gradually going into the energy range of the band-gap, hence the current it carries drops abruptly. The second confined state is still too high in energy to conduct any significant current at this moment. As the last step, since the second confined state becomes closer to the source Fermi level by further increasing the bias, it can carry more current, therefore, the current will increase similarly to the first positive resistance region.

Moreover, we have also investigated the transmission spectra T(E) in a 2D cut along the transport direction illustrated in Fig. 2(a). The figure shows the presence of sharp resonance-peaks at V_R=0.29 V, which are significantly lower at a bias of 0.30 V, yielding the above-mentioned NDR region. Moreover, as depicted in Fig. 2(b), the charge distribution in the device also shows a significant discharging of the QW in the post-resonance condition, which is consistent with the T(E) profiles.

From the local density of states (LDOS) shown in Fig. 3(a), the corresponding alignment of the discrete states on the source, well, and drain side at the bias of 0.29 V is clear, thus concurring with the I-V characteristics and the sharp transmission peaks discussed previously. The T(E), which is shown superimposed on the LDOS with the red solid line, indicates that these peaks are specifically located at the energies at which there is an alignment of the states at −0.059, 0.096, and 0.355 eV for the bias condition V_R=0.29 V. This alignment is very sensitive to the applied drain bias and vanishes when the bias is increased to the post-resonance voltage, see Fig. 3(c). The corresponding current spectra at Fig. 3(b)-(d) also reveal the resonant tunneling phenomena by the two

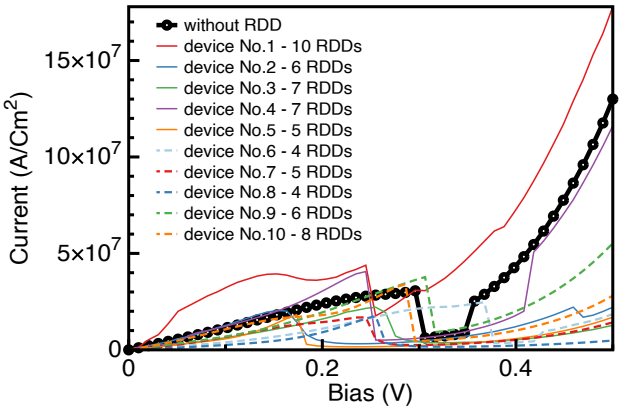

Fig. 4. The I-V characteristics of 10 RTD configurations with RDFs distributed within the RDF region highlighted in Fig. 1 (inset). The baseline structure without any RDFs (smooth device) is presented in black for comparison purposes. It can be seen that devices with the same number of dopants, e.g., No. 6 vs No. 8, No. 5 vs No. 7, No. 2 vs No. 9, and device No. 3 vs No. 4, have a huge variation of V_R.

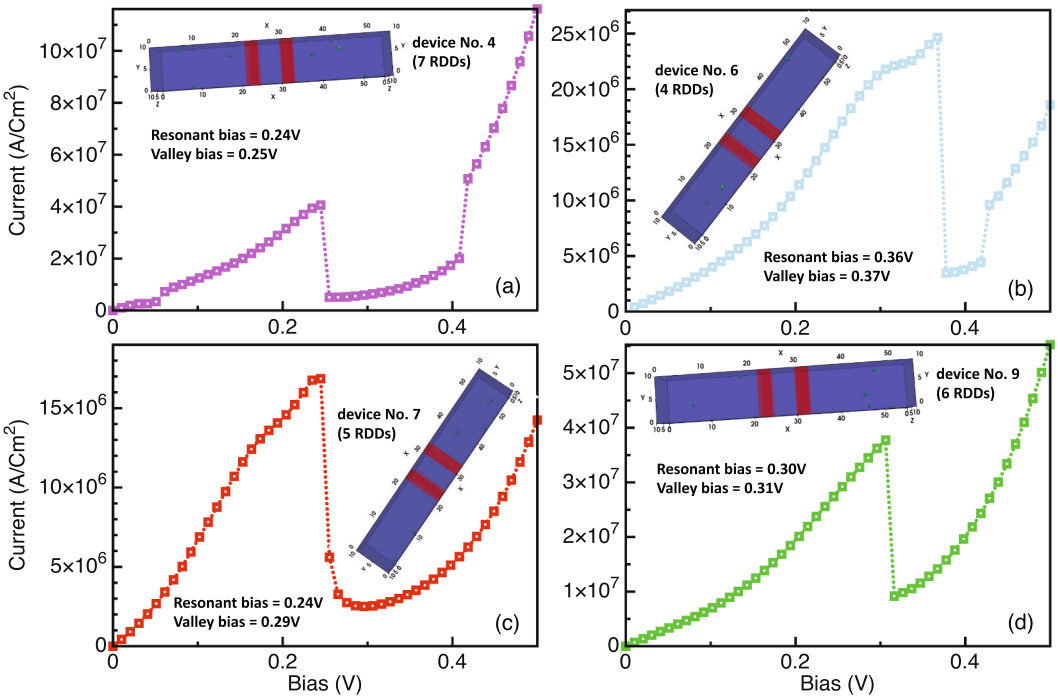

Fig. 5. The I-V characteristics of four random RTD devices in the presence of RDFs, where the insets depict the exact positions of the dopants distributed within the specified RDF region of the structure indicated in Fig. 1. For easier comparison, the line colours are chosen identical to the corresponding curves in Fig. 4.

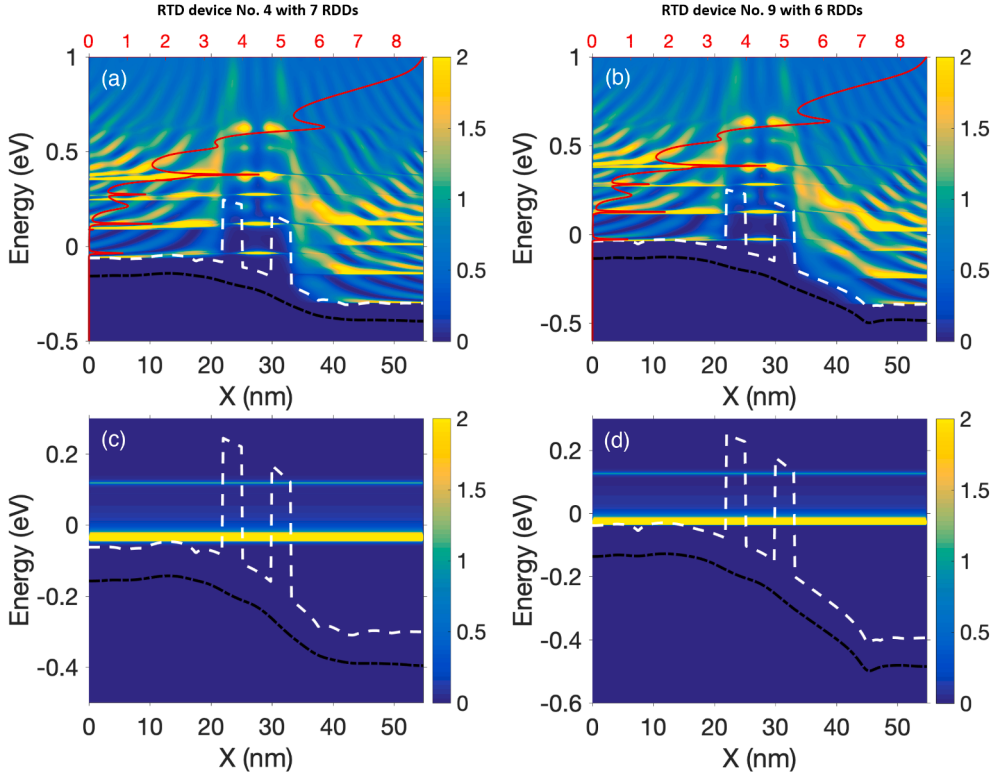

Fig. 6. (a)-(b) The LDOS and T(E) of RTD devices No. 4 and 9, calculated for the bias at which the first resonant-peaks occur (see Fig. 4). Accordingly, the bottom row presents the corresponding energy-resolved current spectra of the aforementioned devices.

very prominent lines at two such aligned energy states and an overall significant and more discrete tunneling current contribution. The tunneling across the potential barriers is also prominent in these simulation results. When the device is driven beyond the resonance condition, it is clearly visible that the current spectra become smaller in magnitude and rather smeared in nature.

Furthermore, we have carried out simulations considering a sample of 10 devices with the unique position of the RDFs to investigate their impact on the V_R (see Fig. 4). In Fig. 5, we look closely at four of those samples and confirm in the insets that devices No. 4, 6, 7, and 9 contain

respectively 7, 4, 5, and 6 dopants each but with a different and unique 3D spatial distribution located within the RDF region. Comparing their I-V characteristics with the smooth (without RDFs) device presented in Fig. 1, we see that there is a direct link between the number and positions of the RDFs and the position of the resonant-peak, position of the valley, and magnitude of the simulated current. Therefore, making them distinguishable from one another in terms of the output I-V characteristics. Hence, these unique I-V characteristics of each device can be used as a unique fingerprint which is determined by characteristics and the material parameters, and thereby cannot be cloned or duplicated for counterfeiting purposes.

Lastly, Fig. 6 shows the energy sub-band structure, transmission spectra, LDOS, and current spectra of two of the aforementioned devices. In terms of the sub-band structures (white dashed line) and the average potential (solid black line), the changes due to the number and position of dopants are very much visible. We also see that the T(E), plotted as a solid red line, spikes at different energy levels, and also the current conduction through the channels has different weights for each case. The significant differences in terms of the potential, band alignment condition, and the transmission spectra all reflect the variations in the I-V characteristics of these devices and therefore display how the quantum nature of the resonance condition can be significantly altered with RDFs variability in these III-V nanowire RTD structures.

4. Conclusion

In summary, we have reported quantum mechanical simulation, utilizing ballistic Non-equilibrium Green's Function (NEGF) approach, of double-barrier III-V resonant tunneling diodes (RTDs) based on nanowire structures. focusing on the influence of random dopant fluctuations (RDFs), we have simulated an ensemble of 10 devices, each with a different and specific RDF distribution. we have shown that the quantum nature of the resonance condition can be significantly altered due to the RDFs. Our software NESS can indeed be used to predict and tailor RTDs behaviour for various future applications such as tunable THz communications, 5G/6G technology, and PUFs.

Declaration of Competing Interest

The authors declare that they have no known competing financial interests or personal relationships that could have appeared to influence the work reported in this paper.

Acknowledgment

This research was funded by Engineering and Physical Sciences Research Council (EPSRC), grants numbers EP/S001131/1 and EP/P009972/1. The authors would like to thank Dr. Nagy, Dr. Carrillo-Nuñez, Dr. Lee, Dr. Berrada, Dr. Badami, and Dr. Duan for their contributions to NESS.

References

[1] Feiginov M. Frequency limitations of resonant-tunnelling diodes in sub-thz and thz oscillators and detectors. J Infrared Milli Terahz Waves 2019;40:365–94. https://doi.org/10.1007/s10762-019-00573-5.
[2] Kasagi K, Suzuki S, Asada M. Large-scale array of resonant-tunneling-diode terahertz oscillators for high output power at 1 thz. J Appl Phys 2019;125:151601. https://doi.org/10.1063/1.5051007.
[3] Biegel BA, Plummer JD. Comparison of self-consistency iteration options for the wigner function method of quantum device simulation. Phys Rev B 1996;54:8070–82. https://doi.org/10.1103/PhysRevB.54.8070.
[4] Biegel B, Plummer J. Applied bias slewing in transient wigner function simulation of resonant tunneling diodes. IEEE Trans Electron Devices 1997;44:733–7. https://doi.org/10.1109/16.568033.
[5] C. Böhm, M. Hofer, Physical Unclonable Functions in Theory and Practice, Springer, New York, NY, 2013, pp. 69–86. doi:10.1007/978-1-4614-5040-5.
[6] Gao Y, Ranasinghe DC, Al-Sarawi SF, Kavehei O, Abbott D. Emerging physical unclonable functions with nanotechnology. IEEE Access 2016;4:61–80. https://doi.org/10.1109/ACCESS.2015.2503432.
[7] McGrath T, Bagci IE, Wang ZM, Roedig U, Young RJ. A puf taxonomy. Appl Phys Rev 2019;6:011303. https://doi.org/10.1063/1.5079407.
[8] Papakonstantinou I, Sklavos N. Physical Unclonable Functions (PUFs) Design Technologies: Advantages and Trade Offs. Cham: Springer International Publishing; 2018. https://doi.org/10.1007/978-3-319-58424-9. pp. 427–442.
[9] Roberts J, Bagci I, Zawawi M, Sexton J, Hulbert N, Noori Y, Young M, Woodhead C, Missous M, Migliorato M, Roedig U, Young R. Using quantum confinement to uniquely identify devices. Sci Rep 2015;5:16456. https://doi.org/10.1038/srep16456.
[10] Bagci IE, McGrath T, Barthelmes C, Dean S, Gavito RB, Young RJ, Roedig U. Resonant-tunnelling diodes as puf building blocks. IEEE Trans Emerging Topics Comput 2021;9:878–85. https://doi.org/10.1109/TETC.2019.2893040. url: https://doi.org/10.1109/TETC.2019.2893040.
[11] Berrada S, Carrillo-Nunez H, Lee J, Medina-Bailon C, Dutta T, Badami O, Adamu-Lema F, Thirunavukkarasu V, Georgiev V, Asenov A. Nano-electronic simulation software (ness): A flexible nano-device simulation platform. J Computat Electron 2020;19. https://doi.org/10.1007/s10825-020-01519-0.
[12] Medina-Bailon C, Badami O, Carrillo-Nuñez H, Dutta T, Nagy D, Adamu-Lema F, Georgiev VP, Asenov A. Enhanced capabilities of the nano-electronic simulation software (ness), in. International Conference on Simulation of Semiconductor Processes and Devices (SISPAD) 2020;2020:293–6. https://doi.org/10.23919/SISPAD49475.2020.9241594.
[13] Medina-Bailon C, Dutta T, Rezaei A, Nagy D, Adamu-Lema F, Georgiev VP, Asenov A. Simulation and modeling of novel electronic device architectures with ness (nano-electronic simulation software): A modular nano tcad simulation framework. Micromachines 2021;12. https://doi.org/10.3390/mi12060680.
[14] Medina-Bailon C, Dutta T, Adamu-Lema F, Rezaei A, Nagy D, Georgiev VP, Asenov A. Nano-electronic simulation software (ness): A novel open-source tcad simulation environment. J Microelectron Manuf 2020;3:20030404. https://doi.org/10.33079/jomm.20030404.
[15] Dutta T, Medina-Bailon C, Rezaei A, Nagy D, Adamu-Lema F, Xeni N, Abourrig Y, Kumar N, Georgiev VP, Asenov A. Tcad simulation of novel semiconductor devices. In: 2021 IEEE 14th International Conference on ASIC (ASICON); 2021. p. 1–4. https://doi.org/10.1109/ASICON52560.2021.9620465.
[16] Jin S, Park YJ, Min HS. A three-dimensional simulation of quantum transport in silicon nanowire transistor in the presence of electron-phonon interactions. J Appl Phys 2006;99:123719. https://doi.org/10.1063/1.2206885.
[17] Martin PC, Schwinger J. Theory of many-particle systems. i. Phys Rev 1959;115:1342–73. https://doi.org/10.1103/PhysRev.115.1342.
[18] L.P. Kadanoff, G. Baym, Quantum Statistical Mechanics: Green's Function Methods in Equilibrium and Nonequilibrium Problems, 1st ed., New York, 1962. doi:10.1201/9780429493218.

Ali Rezaei received his Ph.D. (Dr. rer. nat.) in Condensed Matter Physics at the University of Konstanz, Konstanz, Germany, in 2019. In August 2020, he joined the Device Modelling Group, School of Engineering at the University of Glasgow as a Postdoctoral Research Associate to focus primarily on the further development and expanding the functionality of the non-equilibrium Green's function (NEGF) quantum transport module of NESS.

Amretashis Sengupta received the Ph.D. (Engg.) degree from Jadavpur University, Kolkata, India, in 2012. He carried out his post-doctoral research from the University of Bremen, Germany and the University of Glasgow, UK. He received the DST INSPIRE Faculty Award in 2013, the Hanse-Wissenschaftskolleg fellowship in 2016 and the SERB Research Scientist fellowship in 2020. Currently he is an Associate Professor in the Department of Physics, School of Applied Sciences, REVA University, Bengaluru, India.

Tapas Dutta received the Ph.D. degree in nanoelectronics and nanotechnology from the Grenoble INP, France in 2014. He was with IIT Kanpur, India as a postdoctoral researcher during 2014-17. Since September 2017, he has been with the Device Modeling Group at the University of Glasgow, where he has been a co-developer of NESS (Nano Electronic Simulation Software). His research interests are TCAD software development, and compact modeling of emerging electronic devices.

Cristina Medina-Bailon received the Ph.D. in Electronics from the Univ. of Granada, Spain, in 2017. Her current research interests focus on the Monte Carlo description of tunneling phenomena and on the implementation of classical and semi-classical approaches. In July 2017, she joined the Device Modelling Group at the University of Glasgow as Post-doctoral fellow and she is the software coordinator of NESS since March 2019.

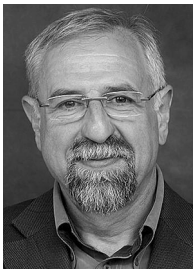

Asen Asenov received the Ph.D. degree in solid-state physics from the Bulgarian Academy of Sciences, Sofia, Bulgaria, in 1989. He was a Chief Executive Officer with Gold Standard Simulations, Ltd., Glasgow, U.K. Currently, he is a James Watt Professor of Electrical Engineering with the University of Glasgow.

Vihar P. Georgiev received his Ph.D. degree from the University of Oxford, Oxford, U.K., in 2011. In 2011, he joined the Device Modelling Group, School of Engineering, University of Glasgow, where he was a Research Associate until 2015 and currently a Senior Lecturer in electronics and nanoscale engineering. He is also UKRI EPSRC innovation fellow.